

IV tester integrated electroluminescence imaging in industrial Si solar cell production

Words: Dr. K. Ramspeck, Dr. S. Fischer, S. Schenk, S. Zimmermann, Dr. M. Alt
h.a.l.m. elektronik GmbH

Electroluminescence (EL) imaging, as a versatile tool for spatially resolved defect analysis on Si-solar cells, has recently gained a lot of traction in its industrial application. In this article we discuss quality control and process control abilities of this technology and how it is applied in solar cell production. We demonstrate how an *IV* tester-integrated solution is ideally suited to increase quality and yield and correlate the EL-data easily with *IV* results.

Quality requirements for solar cells are constantly rising. Besides the current-voltage (*IV*) measurement as sole end of line quality control tool so far, it becomes necessary to detect deficiencies which do not significantly affect the *IV* measurement, such as e.g. cracks.

The minority charge carrier concentration can be converted into the junction voltage [3], which is either governed by the above mentioned recombination processes or by series resistance between the current terminals and the position at which radiation is emitted. The spatially resolved intensity of light emission is captured by a CCD or CMOS camera, resulting in images in which defects appear as darker regions. Therefore, EL imaging is capable of visualising all defects induced by recombination as well as series or parallel resistance. Whereas, a lot of scientific work has previously been dedicated to deriving

quantitative maps of cell parameters like J_{01} or series resistance from EL images (e.g. [1-6]), image analysis approaches implemented in solar cell production focus on extracting position, size, shape and severity of individual defects on solar cells.

Setting up EL imaging is relatively simple. From a hardware point of view, it only requires contacting the cell in a dark environment, a power supply to provide a forward bias and detecting the emitted light with a suitable camera with high sensitivity in the near infrared. Due to recent improvements in cell efficiency and cameras, short measurement times below 120 ms already yield a low-noise high-resolution image.

Giving information on all relevant defects and being relatively simple to implement, EL imaging recently evolved from a laboratory diagnosis tool to a widely used

tool in end-of-line testing of solar cells and modules.

Its main applications in solar cell production are quality sorting and identification of processes that cause defects. For quality sorting, cells containing different defects exceeding a certain severity shall be sorted into lower quality bins. For the detection of deficient production steps, statistics on different defect categories are required. To obtain the relevant numbers, typically an EL evaluation pipeline is implemented (figure 1). In the first step, the image is recorded using optimised hardware settings including gain, image acquisition time and bias applied to the cell under evaluation. Step 2 comprises image pre-processing such as rectification, defect pixel removal or filtering. In step 3, segmentation of the pre-processed image and feature extraction provide a list of defect candidates and their features. Filtering of defect candidates based on their features provides the defects of interest in step 4. Finally, the last step comprises an evaluation of the EL information of the whole cell under test in order to assign a BIN class. Please note that the image analysis techniques employed for the different steps might differ between implementations.

As a leading manufacturer of *IV* measurement equipment, h.a.l.m. elektronik GmbH has integrated the EL imaging system with the *IV* tester into one end-of-line characterisation platform (figure 2). The EL camera is mounted at the flash box, and the

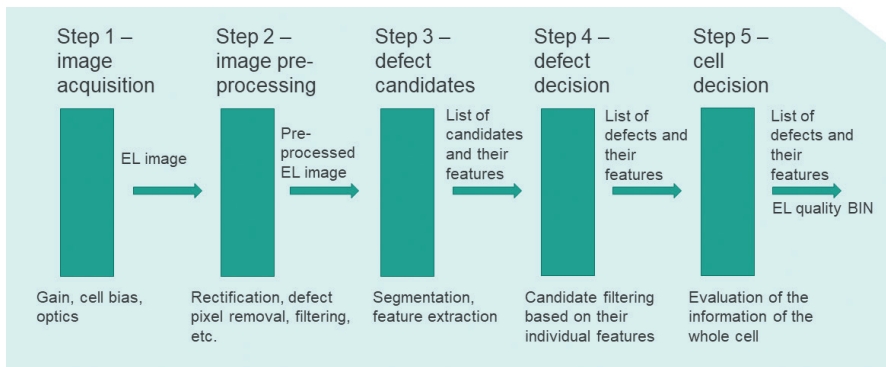


Figure 1: Scheme of a typical EL evaluation process flow, showing the different steps in the process of obtaining statistics on individual defects and defining a quality BIN for a solar cell from an EL image.

The ability to measure any kind of defect makes EL a mighty tool, but leads to challenges in rigorously defining quality criteria and discriminating the different root causes of visible defects. The main challenge is an unambiguous formulation of the requirements for the different quality grades, including definitions for all occurring defects in all their representations. Since most defects occur with different severities as shown for one example in figure 3, the line between different quality grades is intrinsically difficult to define.

EL image is acquired in one measurement sequence together with the IV curves. The system is equipped with automatic defect detection algorithms in the image analysis software package PVControl-EL-eval 2.0 ready for usage with all common cell types.

Acquiring IV data and an EL image without re-contacting the solar cell saves floor-space, contacting equipment and (most importantly) reduces breakage rates. Furthermore, the results from EL imaging and IV testing are collected in one database. This enables combined analysis approaches of EL and IV results and statistical data analysis to correlate EL defects and their severity with IV data anomalies. We expect such integrative data correlation approaches to become more common in the PV industry in future, particularly in the context of

self-adjusting maintenance concepts for smart PV factories.

PVControl-EL-eval 2.0 incorporates two concepts that can be combined or applied separately for solar cell quality and process control. Individual defects of different classes are extracted, visualised in an overlay image and their features such as count, area and severity are measured and stored. Application of thresholds to these features provides a basic sorting of cells into quality bins. However, the requirements for solar cell sorting are typically more complex and they are individual for each factory or at least for each company. Furthermore, they evolve as the production process changes. For this purpose, h.a.l.m. offers a cell sorting configuration that is specific to each customer.

A close cooperation of EL system supplier and solar cell manufacturer is therefore required, as the quality BIN definition typically cannot be described in a clear written specification. For determining the BIN definition, it is particularly difficult to set the cell grade for cells with defects of intermediate severity. According to our experience, the decision for such cells is so difficult that it depends on the person taking it or even varies if the same person assesses the same cell twice. The most reliable way to achieve a well-defined boundary between the different quality grades is sorting a batch of representative images by at least three trained employees of the solar cell manufacturer. The batch has to contain a sufficient number of images of cells with all defects that occur in the factory as well as images of cells without defects. Combining the rating from three experts consolidates clear assignments to quality bins and demonstrates in which cases it is not



Batch: Classification | Monitor cell | IV diagram | Flasher:XF2 | Machine statistics | Electroluminescence

PVControl - Batch Administration

h.a.l.m. cetisPV product line

Operation mode: Automatic | Manual | Serial measurement | Maintenance

Manual measurement: Start | Abort | Status: Manual measurement ready | Info

Login: Title: test | Comment: | Cell ID: | User: halim | Recipe: Default_1Level_20ms

Results: [Q1] IV-Curve in light | [Q1], [Q2], [Q3], [Q3H] | [Q1] light [Q3H] dark | [EL] | [ALL]

Results Summary:

- Isc [A]: 9.658 | ELMeanGra: 111
- Uoc [V]: 0.663 | EL2CrackDx: 1
- FF [%]: 80.867 | EL2FingerD: 3
- Eta [%]: 21.679 | EL2FingerC: -
- Rser [Ohm]: 0.002 | EL2DarkDel: 2.551
- Rsh [Ohm]: 43.088 | EL2DarkDel: 24
- IRev2 [A]: 1.834 | EL2EvalGrad: 1.000
- EL2Class [%]: 87.226

Statistics / trends: Results | Results-Statistics | Results-BIN-Statistics | Trends Isc, Pmpg, FF | Trends Uoc, FF, Eta | Trends BIN, FF, Incol

TestTime	TestDate	Comment	Bin	Isc [A]	Uoc [V]	Pmpg [W]	Eta [%]	FF [%]	Incol [W/m²]	RserL [Ohm]	RshumL [Ohm]	Tecl [°C]	Tmonecl [°C]	Rser [Ohm]
245	10:27:28	28-03-2018	20	9.60793	0.66559	5.1215	21.43	79.44	999.70	-	13.999	22.84	22.29	0.00221
246	10:27:47	28-03-2018	20	9.68511	0.66585	5.0963	21.33	79.05	1000.28	-	11.524	22.72	22.18	0.00248
247	10:28:16	28-03-2018	20	9.68172	0.66590	5.1388	21.50	79.67	1001.13	-	10.830	22.93	22.18	0.00195
248	10:28:18	28-03-2018	20	9.68516	0.66595	5.1400	21.51	79.69	1000.01	-	11.822	22.57	22.25	0.00197
249	10:13:48	28-03-2018	20	9.68442	0.66259	5.1420	21.52	80.13	1000.65	-	160.071	22.63	22.25	0.00232
250	10:14:35	28-03-2018	20	9.68463	0.66271	5.1472	21.54	80.20	1000.47	-	78.330	22.94	22.28	0.00225
251	10:14:52	28-03-2018	20	9.68259	0.66200	5.1452	21.53	80.18	1000.94	-	59.795	23.03	22.28	0.00226
252	10:15:14	28-03-2018	20	9.68202	0.66308	5.1638	21.61	80.43	1000.57	-	64.963	23.21	22.28	0.00205
253	10:15:51	28-03-2018	20	9.70820	0.66420	5.1912	21.73	80.51	1000.80	-	50.013	22.92	22.27	0.00205
254	10:16:38	28-03-2018	20	9.70567	0.66428	5.1737	21.85	80.25	1000.41	-	51.438	23.19	22.28	0.00221
255	10:16:50	28-03-2018	20	9.70396	0.66472	5.1934	21.73	80.51	999.73	-	33.730	23.34	22.32	0.00199
256	10:17:13	28-03-2018	20	9.70147	0.66475	5.1913	21.73	80.50	999.98	-	44.661	23.22	22.31	0.00197
257	10:17:20	28-03-2018	20	9.70115	0.66471	5.1898	21.71	80.46	999.41	-	48.921	23.22	22.31	0.00198
258	10:17:50	28-03-2018	20	9.68885	0.66524	5.1778	21.67	80.33	999.84	-	39.716	22.97	22.31	0.00214
259	10:18:29	28-03-2018	20	9.68814	0.66524	5.1911	21.68	80.39	1000.25	-	57.704	23.98	23.31	0.00208
260	10:21:51	28-03-2018	20	9.66251	0.66295	5.1772	21.67	80.82	999.72	-	78.150	22.73	22.42	0.00196
261	10:28:34	28-03-2018	20	9.65816	0.66325	5.1801	21.68	80.57	1000.20	-	43.688	23.04	22.43	0.00189

Status: Operation mode changed: Manual | Operation mode changed: Maintenance | Operation mode changed: Manual | Operation mode ch...

Figure 2: Setup of the h.a.l.m. IV tester with integrated EL system. The electroluminescence camera is mounted at the flash box of the IV measurement system and the software displays IV and EL results together.

possible to agree on a cell grade. This process allows deducing for which cells the decision is clear and unambiguous as well as sorting cells into the correct quality BIN if the decision is more complex. Based on the specification, a customer specific recipe for the automatic defect detection with PVControl-EL-eval is tuned.

In addition to improving the cell quality by sorting out defective cells, process optimisation and even concepts of automatic maintenance are supported by a well mastered automatic defect analysis. This is especially the case if defects are correlated with IV data cell wise, as given by the cetisPV-EL-package. The combination of quality sorting and the detection of individual defects, which cause quality issues, allows a feedback to the processes that are responsible for them (figure 4).

Mapping of e.g. gripper marks to the position of the responsible gripper in the solar cell production line thus becomes possible using the entire information on the defect, provided by the analysis software. In this way, processes can be optimised and tuned to reach higher yields, manually in the present and automatically in the future after clear correlations with the process steps have been identified in the production facilities.

In conclusion, electroluminescence imaging allows a decent increase in product quality and yield in solar cell production, providing spatially resolved information on defects which affect initial efficiency or may lead to degradation or breakage at a later stage. Exploiting its capabilities in an integrated measurement station together with the IV tester and providing best-in-class automatic defect detection, the cetisPV-EL-package together with PVControl-EL-eval 2.0 provides a smart solution to benefit from EL imaging in solar cell production and to make the factory ready for the future.

www.halm.de

References:

[1] T. Fuyuki, H. Kondo, T. Yamazaki, Y. Takahashi and Y. Uraoka, *Appl. Phys. Lett.* 86, 262108 (2005)
 [2] U. Rau, *Phys. Rev. B* 76, 085303 (2007)
 [3] K. Bothe, P. Pohl, J. Schmidt, T. Weber, P. Altermatt, B. Fischer and R. Brendel, *Proc. of the 21st EU-PVSEC*, p 597 - 600 (2006), Dresden, Germany
 [4] O. Breitenstein, A. Khanna, Y. Augarten, J. Bauer, J.-M. Wagner and K. Iwig, *Phys. Status Solidi RRL*, 4, 1, p. 7-9 (2010)
 [5] J. A. Giesecke, M. Kasemann, M.C. Schubert, P. Würfel and W. Warta, *Prog. In Photovoltaics: Res. And Appl.*, 18, p.



Figure 3: EL images showing cells with contact formation defect with increasing severity level. At the top, the defect is almost not visible, while the last cell at the bottom shows a clear, large, almost black region.

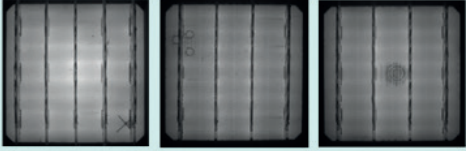
Process step	Defect type	Examples
Wafer Czochralski process / Ingot crystallization process	Oxidation ring Dark grain boundary Edge brick	
Cell Handling	Crack Gripper mark	
Front side metallization	Finger defect	
Contact formation process	Insufficient formation	
IV measurement	Inhomogeneous contacting	

Figure 4: Examples of correlation between EL-visible defects and solar cell processing steps.

10-19 (2010)

[6] T. Trupke, R.A. Bardos, M.D. Abott, P. Würfel, E. Pink, Y. Augarten, F.W. Chen, K. Fisher, J.E. Cotter, M. Kasemann, M. Rüdiger, S. Kontermann, M.C. Schubert, M.

The, S.W. Glunz, W. Warta, D. Macdonald, J. Tan, A. Cuevas, J. Bauer, R. Gupta, O. Breitenstein, T. Buonassisi, G. Tarnowski, A. Lorenz, H.P. Hartmann, D.H. Neuhaus, J.M. Fernandez, *Proc. of the 22nd EU-PVSEC*, p. 22 – 30 (2007), Milan, Italy